Atmos. Chem. Phys. Discuss., 11, 7781–7809, 2011
www.atmos-chem-phys-discuss.net/11/7781/2011/
doi:10.5194/acpd-11-7781-2011
© Author(s) 2011. CC Attribution 3.0 License.

Atmospheric Chemistry and Physics Discussions

This discussion paper is/has been under review for the journal Atmospheric Chemistry and Physics (ACP). Please refer to the corresponding final paper in ACP if available.

Branch-level measurement of total OH reactivity for constraining unknown BVOC emission during the CABINEX (Community Atmosphere-Biosphere INteractions Experiments)-09 Field Campaign

S. Kim, A. Guenther, T. Karl, and J. Greenberg

ACD/NESL NCAR, P.O. Box 3000, Boulder CO, 80307, USA

Received: 2 March 2011 – Accepted: 3 March 2011 – Published: 7 March 2011

Correspondence to: S. Kim (saewung@ucar.edu)

Published by Copernicus Publications on behalf of the European Geosciences Union.

Abstract

We present OH reactivity measurements using the comparative reactivity method with a branch enclosure technique for four different tree species (red oak, white pine, beech and red maple) in the UMBS PROPHET tower footprint during the Community Atmosphere Biosphere INteraction EXperiment (CABINEX) field campaign in July of 2009. Proton Transfer Reaction-Mass Spectrometry (PTR-MS) was sequentially used as a detector for OH reactivity and BVOC including isoprene and monoterpenes (MT), in enclosure air, so that the measurement dataset contains both measured OH reactivity and calculated OH reactivity from well-known BVOC. The results indicate that isoprene and MT, and in one case a sesquiterpene, can account for the measured OH reactivity. Significant discrepancy between measured OH reactivity and calculated OH reactivity from isoprene and MT is found for the red maple enclosure dataset but it can be reconciled by adding reactivity from emission of a sesquiterpene, α-farnesene, detected by GC-MS. This leads us to conclude that no significant unknown BVOC emission contributed to ambient OH reactivity from these trees at least during the study period. This conclusion leads us to explore the contribution from unmeasured isoprene (the dominant OH sink in this ecosystem) oxidation products such as hydroxyacetone, glyoxal, methylglyoxal and C4 and C5-hydroxycarbonyl using recently published isoprene oxidation mechanisms (Mainz Isoprene Mechanism II and Leuven Isoprene Mechanism). Evaluation of conventionally unmeasured first generation oxidation products of isoprene and their possible contribution to ambient missing OH reactivity indicates that the ratio of OH reactivity from unmeasured products over OH reactivity from MVK + MACR is strongly dependent on NO concentrations. The unmeasured oxidation products can contribute ~7.2% (8.8% from LIM and 5.6% by MIM 2 when NO = 100 pptv) of the isoprene contribution towards total ambient OH reactivity. This amount can explain ~8.0% (9.7% from LIM and 6.2% from MIM 2) of missing OH reactivity, reported by Di Carlo et al. (2004) at the same site. Further study on contribution from further generation of unmeasured oxidation products should be followed to constrain tropospheric

ACPD

11, 7781–7809, 2011

photochemical reactivity of BVOC that have important implications for both photochemical ozone and secondary organic aerosol formation.

1 Introduction

Total OH reactivity is defined as the quantity of total atmospheric constituents that can react with OH with reactivity scale units of s^{-1}. It is equivalent to the inverse of the lifetime of OH in the presence of those atmospheric constituents. The measurement results have provided quantitative information about how well we constrain reactive constituents in the atmosphere by comparing total calculated OH reactivity, represented by the sum of products between each measured concentration of reactive constituents in the atmosphere and the reaction constant with OH of the given constituent. Lou et al. (2010) summarized the ratios of measured and calculated total OH reactivity reported in the range of 1 to 3 from 16 field campaigns. The higher ratios were often observed in rural and forested areas, where biogenic volatile organic compounds (BVOC) are a dominant player in regional photochemistry. The unaccounted measured OH reactivity relative to calculated OH reactivity is often called "missing OH reactivity". This higher degree of missing OH reactivity in BVOC dominant regions strongly suggests significant uncertainty in constraining BVOC and their oxidation products in the atmosphere. Considering the dominance of BVOC emission relative to anthropogenic VOC emission (ten times higher; Goldstein and Galbally, 2007), this uncertainty can be a potential problem in understanding photochemical ozone and secondary organic aerosol (SOA) formation in the atmosphere, two important radiative forcing agents controlling global climate (IPCC, 2007). For this reason, a number of studies have tried to identify the sources of unexplored reactive compounds in BVOC dominated regions. The potential sources include (1) unmeasured reactive BVOC emissions, (2) unmeasured reactive oxidation products from known BVOC such as isoprene and monoterpenes (MT), and (3) uncertainties in measured OH reactivity, BVOC and their reaction rates. Existence of unmeasured BVOC emission is supported by evidence such as:

ACPD
11, 7781–7809, 2011

(1) temperature dependence of missing OH reactivity closely following the temperature dependence of terpenoid emission (Di Carlo et al., 2004) (2) high sesquiterpene emissions from some ecosystems that are very reactive and have not been constrained by measurements (Bouvier-Brown et al., 2009) and (3) total MT concentrations, measured by the gas-chromatography technique (GC-FID) being consistently lower than those measured by proton transfer reaction mass spectrometry (PTR-MS; Lee et al., 2005).

On the other hand, other studies have shown that (1) ambient sesquiterpene concentrations at the PROPHET site, where significant missing OH reactivity was reported, were too low to explain the missing OH reactivity (Kim et al., 2009), (2) missing OH reactivity could be reconciled by the addition of unmeasured oxidation products estimated with a box model calculation (Lou et al., 2010), (3) new oxidation mechanisms of isoprene elucidate faster production of conventionally unmeasured oxidation products (Karl et al., 2010; Paulot et al., 2009), and (4) there is good agreement between sensitivity-corrected PTR-MS mass spectra observed in ambient air with those from branch enclosures (Kim et al., 2010). These study results strongly suggest that the source of unknown reactive species in the atmosphere, in at least some of these locations, is poorly constrained oxidation products rather than unconstrained emitted species.

To directly constrain the source of missing reactive species, we conducted total OH reactivity measurement with a branch enclosure for four different tree species in the PROPHET tower ecosystem, an isoprene dominated ecosystem, during the Community Atmosphere-Biosphere Interaction Experiment (CABINEX) field campaign in July, 2009. In this ecosystem, a significant amount of missing OH reactivity was reported by Di Carlo et al. (2004). In this study, we used the comparative reactivity method (CRM, Sinha et al., 2008) to measure total OH reactivity of emissions from individual branches using proton transfer reaction-mass spectrometry (PTR-MS). The PTR-MS system was also used to monitor BVOC concentrations inside of the enclosure to calculate total OH reactivity from known biogenic emissions such as isoprene and MT. The comparison between the measured and the calculated total OH reactivity gives us an opportunity

ACPD
11, 7781–7809, 2011

to quantitatively assess the contribution of missing OH reactivity from unknown BVOC emission. We also present calculation results using two up-to-date isoprene oxidation mechanisms (Mainz Isoprene Mechanism 2 (MIM2) Taraborrelli et al., 2009 and Leuven Isoprene Mechanism (LIM) Stavrakou et al., 2010) to assess possible contributions of unmeasured isoprene oxidation products towards total OH reactivity.

1.1 Methods

1.2 Branch enclosure-CRM OH reactivity measurement system

The schematic diagram of the measurement system deployed for the CABINEX field campaign is shown in Fig. 1. The CRM method to measure total OH reactivity is thoroughly described in Sinha et al. (2008) and the potential interferences from water vapor variations are discussed in Sinha et al. (2009). We, therefore, provide a brief overview of the principle of the measurement as follows:

- Step 1 A known amount of pyrrole (C_4H_4NH) is introduced into the glass reactor along with VOC free air, which has passed through the catalytic converter. The pyrrole signal is monitored by PTR-MS.
- Step 2 The UV lamp is turned on to generate OH from humidified UHP nitrogen. The pyrrole signal is expected to decrease because of rapid reaction with OH ($k_{OH-Pyrrole} = 1.2 \times 10^{-10}\,cm^3\,molecule^{-1}\,s^{-1}$).
- Step 3 Sample air from the enclosure is introduced by switching the 3-way valve in Fig. 1. The pyrrole signal from Stage 2 will be increased due to OH reaction competition with reactive constituents (mostly BVOC) in the sample air. Total OH reactivity of the sample air can be calculated from the signal differences as described in Sinha et al. (2008).
- Step 4 The UV lamp is turned off and isoprene and MT in the sample air are analyzed with PTR-MS to assess the contribution of these compounds to the measured total OH reactivity.

ACPD
11, 7781–7809, 2011

– In step 2, the pyrrole concentration inside of the glass reactor was maintained at 30 ppbv, significantly higher than the concentration of OH (~2 ppbv) to achieve the pseudo first order reaction regime so that total OH reactivity is only linearly dependent on the pyrrole concentration variation and independent of the OH concentration.

Since PTR-MS is only able to measure total MT concentration rather than speciated MT concentration, which are required to calculate the precise contribution of OH reactivity from MT, occasional sorbent cartridge (Tenax GR and Carbograph 5TD, Markes Int., Llanstrisant, UK) sampling was conducted for MT speciation information. In addition, BVOC emission other than isoprene and MT can be detected by the cartridge samplings.Adsorbed VOCs were measured using a Series 2 Ultra^{TM} TD autosampler coupled to a Unity 1 thermal desorption system (MARKES International, Llantrisant, UK) interfaced with a 7890A series Gas Chromatograph/5975C Electron Impact Mass Spectrometer (GCMS) with a triple-axis detector (Agilent Technologies, Santa Clara, CA, USA). The GC was fitted with a DB5 column (0.25 mm ID × 30 m, 0.25 micron stationary phase) and was temperature programmed with an initial hold of 1 min at 35 °C and subsequent temperature rampings of 6 °C min^{-1} to 80 °C, 3 °C min^{-1} to 155 °C, 10 °C min^{-1} to 190 °C, 25 °C min^{-1} to 260 °C with a final hold of 5.2 min. to a final temperature of 300 °C.

The above procedures were conducted according to a programmed routine. The volume of the Teflon branch enclosure was around 3 l and the ozone and VOC scrubbed air was introduced at the rate of ~6 l min^{-1}. Temperature inside of the enclosure was monitored and logged by K-type thermocouple with a portable data logger (HOBO, Onset, Pocasset, MA), Photosynthetically Active Radiation (PAR) above the enclosure was also measured using a Line Quantum Sensor (LI-191, LI-COR Lincoln, NE) and the signal was also logged with a portable data logger (HOBO, Onset, Pocasset, MA). After enclosing a branch, we waited one day before starting the measurement in order to minimize sampling of disturbed emissions (Kim et al., 2010).

ACPD
11, 7781–7809, 2011

1.3 Laboratory calibration

Before and after the field campaign, we tested the system response over a wide range of total OH reactivity. A standard gas mixture with methanol, acetonitrile, acetaldehyde, acetone, isoprene, methyl vinyl ketone, benzene, toluene, and camphene (1 ppmv ± 5%, NCAR) was mixed with zero air to generate standard samples for multipoint OH reactivity calibrations. The calibration results are summarized in Fig. 2, indicating excellent linearity over a wide range of reactivity. The limit of detection is about 15 s^{-1} for a five minute averaging time from the signals at Step 2 using Poisson statistics (3σ), which are routinely used to assess limit of detections for chemical ionization mass spectrometry techniques (Kim et al., 2009). For this study, there was no attempt to lower the detection limit because the enclosure sample was expected to have much higher OH reactivity than the assessed detection limit. Readers who are interested in ambient measurements requiring lower detection limits are referred to Sinha et al. (2010).

1.4 Enclosure total OH reactivity measurement results and comparisons with calculated total OH reactivity from known BVOC (isoprene and monoterpenes)

Total OH reactivity measurements of enclosed branches were conducted during the whole month of July of 2010. Climatologically, the experimental period was characterized by below normal temperature and above normal precipitation. Branches for enclosure measurements were selected on trees near the lab in order to reduce wall loss of potential reactive emission compounds. This constraint allowed us to sample only the understory branches.

Ortega et al. (2007) reported specific tree species composition near the PROPHET tower ecosystem and isoprene and MT basal emission rates of the five major tree species. The study reported red oak (Quercus rubra) as one of dominant isoprene emitters and white pine (Pinus strobus) as one of most dominant MT emitters in this

ACPD
11, 7781–7809, 2011

ecosystem. The daily variations of measured and calculated total OH reactivity for the oak tree branch enclosure are presented in the bottom panel of Fig. 3 along with branch enclosure temperature and PAR variations in the upper panel. In addition, the composition of BVOC, which was measured by sorbent cartridge sampling with GC-MS/FID analysis, from the oak tree enclosure is summarized in Table 1. The data for the first three days were from one branch enclosure system (Oak Branch 1) and the data of 24 July was from another branch (Oak Branch 2). The variations of measured OH reactivity can be reasonably explained by the calculated OH reactivity variations from isoprene concentrations measured by PTR-MS except on 5 July. For comparison purposes, in Fig. 4, afternoon temporal variations (2 p.m. to 6 p.m.) of measured and calculated OH reactivity are presented for 4 July and 5 July along with enclosure temperature and PAR variations. The temperature and PAR variations of both days appear quite different – 4 July has a typical daily temperature evolution for no cloud conditions but the variation on 5 July indicates a few abrupt temperature changes just after the temperature reached the peak temperature of the day due to clouds blocking solar radiation. The differences in the measured and calculated OH reactivity can be explained by this difference. On 4 July, as temperature smoothly varies, the calculated and measured OH reactivity variations are comparable but on 5 July the temperature drop in the middle of the day causes a depressed measured OH reactivity, which was caused by decreased terpenoid emissions. However, as the enclosure temperature increased while the system was operated in the BVOC measurement mode, the calculated OH reactivity indicated a big increase. Shortly after, the temperature dropped off again, while the system changed to the OH reactivity measurement mode. These differences are also confirmed by PAR variations, also plotted in Fig. 4. Thus, we can understand that the significant disagreement on 5 July was actually caused by rapidly changing physical parameters that result in calculated and measured OH reactivity measurements that cannot be directly compared. Figure 5 illustrates daily variations of measured and calculated OH reactivity (bottom panel) and enclosure temperature and PAR above the white pine enclosure (upper panel). As summarized in Table 1, MT is

ACPD
11, 7781–7809, 2011

the most dominant BVOC emission of the enclosure and the calculated OH reactivity variations by MT emission are in range of measured OH reactivity variations as shown in Fig. 5.

To quantitatively compare the measured and the calculated OH reactivity for the same conditions of PAR and temperature, the two dominant physical parameters controlling BVOC emission, one-minute averaged measured and calculated OH reactivity were plotted as a function of temperature in Fig. 6. Overall, both the measured and calculated OH reactivity datasets closely followed the exponential function that is expected for the temperature dependence of BVOC emissions (Guenther et al., 1995). A 5 °C running averaged measured and calculated OH reactivity with color-coding of PAR on the plots clearly indicate that the difference of the measured and calculated OH reactivity in the 5 °C temperature bin can be explained by the differences in PAR. This comparison demonstrated the good agreement between measured and calculated OH reactivity. These results suggest that there is no significant missing OH reactivity associated with primary BVOC emission for red oak and white pine, which are the two main tree species dominating isoprene and MT emissions, respectively, in this ecosystem.

The upper panel of Table 2 shows the BVOC composition of a beech tree branch enclosure determined by GC-MS measurement from cartridge sampling. BVOC emission from beech in the PROPHET tower ecosystem was not previously characterized. MTs were the dominant emission of the particular branch investigated and sesquiterpenes (SQT), primarily α-farnesene, composed a minor fraction of the emission. Although we measured two different beech branch enclosures during the study period, the cool and rainy weather resulted in only two days of datasets with detectable emission rates. Overall, temporal variations of the measured and calculated (only MT considered) OH reactivity show reasonable agreement as shown in Fig. 7. The cartridge sampling analysis results, in the bottom panel of Table 2, indicate that the dominant emission from a red maple tree enclosure was α-farnesene. Since α-farnesene is a very reactive compound with OH ($k_{OH} = 3.2 \times 10^{-10}$), this results in an obvious discrepancy between measured and calculated OH reactivity with measured values that are

ACPD
11, 7781–7809, 2011

consistently higher than measured values when the calculated values only consider observed MT concentrations in the branch enclosure as shown in Fig. 8. To take into account α-farnesene contributions towards measured OH reactivity, the ratio of MT and α-farnesene concentrations, observed from sorbent cartridge analysis is used to include SQT in the calculated OH reactivity. The temporal variations of the calculated OH reactivity including SQT, indicated by green triangles in Fig. 8 shows much closer agreement with measured OH reactivity.

To our knowledge, this study is the first published report of direct total OH reactivity measurement using an enclosure technique to constrain missing BVOC emission. Our measurement and data analysis clearly indicate that the temporal variations of branch enclosure OH reactivity measurements of three different tree species can be explained by the variations of calculated OH reactivity from isoprene and MT, and other known BVOC. A fourth species, red maple, had consistently higher measured OH reactivity than could be explained by isoprene and MT but by consideration of the reactivity of a SQT, α-farnesene, we can reconcile the discrepancy between measured and calculated OH reactivity. These results, therefore, do not suggest that there is a significant unknown or unmeasured primary BVOC emission for the tree species that dominate this ecosystem. However, additional branch enclosure OH reactivity measurements are needed to characterize the dominant species in other ecosystems.

1.5 Possible contributions of first generation oxidation products of isoprene to ambient total OH reactivity

If we conclude that there is no significant unknown primary BVOC emission that contributes to OH reactivity, then we must consider if there is any other source of missing OH reactivity in this forest canopy. One possibility is that unmeasured/unknown isoprene oxidation products are responsible since isoprene is the most dominant BVOC emission in this ecosystem. This may be the case since significant uncertainties exist regarding isoprene oxidation products and their yields even though many studies of

ACPD
11, 7781–7809, 2011

isoprene oxidation have characterized kinetics, oxidation products and their yields in laboratories during the past few decades. Paulson and Seinfeld (1992) presented a comprehensive isoprene oxidation mechanism based on studies beginning in the late 70s and results from their chamber experiments. They confirmed that the major first oxidation products of isoprene are methyl vinyl ketone, methacrolein, formaldehyde, and alkyl nitrate under conditions of high NO and estimated that 22% of the carbon was not identified. The candidates of unidentified products were speculated as "multifunctional, mostly five carbon compounds that form via allylic rearrangement." These speculated compounds were tentatively identified by PTR-MS from field experiments (Williams et al., 2001) and laboratory experiments (Zhao et al., 2004). As Paulson and Seinfeld (1992) speculated, the compounds were C4 and C5 hydroxycarbonyl compounds and their yields were estimated to be ~31% (Zhao et al., 2004). These findings catalyzed multi-platform (theoretical, laboratory and field) studies, revealing the complicated nature (e.g. Dibble, 2004a, b, and Paulot et al., 2009) of isoprene oxidation chemistry.

Recently, Karl et al. (2009) assessed a number of isoprene oxidation chemistry mechanisms to explain unexpected high hydroxyacetone concentrations observed in the Amazon forest. Conventionally, hydroxyacetone was considered a major oxidation product of MACR by OH. The production rate of hydroxyacetone from MACR oxidation could only explain 10% of the observed hydroxyacetone. To reconcile the discrepancy, Karl et al. (2009) proposed direct production of hydroxyaetone from isoprene oxidation by OH with a molar yield of 8.3%. Indeed, a number of recent findings from laboratory experiments and theoretical mechanism studies report hydroxyacetone as a first generation oxidation product of isoprene. However, the reported hydroxyacetone yield from isoprene OH oxidation as the first generation product by Paulot et al. (2009) in high NO_X condition is significantly lower (3.8%) than what Karl et al. (2009) proposed. There are several possibilities for this discrepancy. The first possibility is differences in analytical techniques. Paulot et al. (2009) used CF_3O^- ion chemistry to detect oxidation products of isoprene including hydroxyacetone. The second reason could be different NO_X conditions, critically controlling peroxy radical chemistry. This discrepancy

ACPD
11, 7781–7809, 2011

urges more systematic laboratory studies with comprehensive measurement tools with various simulation conditions.

We evaluated possible contributions towards ambient total OH reactivity from recently published isoprene oxidation mechanisms (MIM and LIM), which have been embedded in global 3-D chemical transport models. Both models incorporated the new findings on isoprene oxidation chemistry and show very strong NO dependence in their product distributions (Stavrakou et al., 2010 for LIM and Taraborelli et al., 2009 MIM). From the oxidation product distributions estimated with the model calculation, we calculated total OH reactivity from each case and assessed the fraction from the routinely measured compounds (e.g. MVK and MACR) and the unmeasured compounds (e.g. C5, C4-hydroxycabonyl compounds, hydroxyacetone, glyoxal, glycolaldehyde etc.). Since HPALD1 and HPALD2 (two isomers of C5-hydroperoxyaldehyde) are only present in LIM, the first generation products from the 1.6-H shift of isoprene hydroxylperoxy radicals, have a very short photolysis lifetime ($J = 5 \times 10^{-4}\ s^{-1}$), we regarded photolysis products of HPALD1 and HPALD2 (hydroxyacetone, methylglyoxal, glycolaldehyde, and CH_2O) also as isoprene first generation oxidation products. Based on the isoprene daily variation observed at the PROPHET tower site in the summer of 2005 by PTR-MS, we ran a time-dependent box model to obtain isoprene first generation oxidation product production. Daily variations of OH, HO_2 and RO_2 are constrained by daily maximum concentrations of 2.5×10^6, 1×10^9, and 1×10^9. The daily variation of OH concentration is assumed to follow daily variation of J_{NO_2} from the TUV 4.1 model run for the site. The HO_2, RO_2 daily variations are assumed to be similar with the OH daily variation and the difference from the OH variation maintained at a level of 25% of the daytime maximum before dawn and after sunset (Tan et al., 2001).

The calculation results are presented in Fig. 8. The left panels of the figures show the diurnal variations of OH reactivity from MVK + MACR (red solid) and the unmeasured compounds (red dash) and the ratio of OH reactivity from MVK + MACR and the unmeasured compounds from the LIM oxidation scheme. Each panel shows the simulation with different NO mixing ratios as indicated in the figure. The right panels

ACPD
11, 7781–7809, 2011

of Fig. 8 contain corresponding calculation results from the MIM oxidation scheme. Both schemes predict higher OH reactivity from the unmeasured compounds than OH reactivity from MVK + MACR in a low NO environment. However the ratios of OH reactivity from unmeasured compounds with MVK + MACR indicates significant differences between the mechanisms for different NO levels. Especially for 50 pptv of NO, the LIM scheme indicates that OH reactivity from unmeasured compounds is ~3.2 times higher than that from MVK + MACR. On the other hand, the MIM scheme indicates ~1.5 times higher OH reactivity from unmeasured compounds than OH reactivity from MVK + MACR. It is also noticeable that in the high NO simulation, MIM predicts higher ratios than those from LIM. These exercises suggest that the contribution of conventionally unmeasured oxygenated VOC to total OH reactivity should be carefully evaluated for appropriate NO conditions to constrain the source of missing OH reactivity in clean forest environments where relatively high missing OH reactivity has been reported. These ratios indicate the OH reactivity contribution that first generation unmeasured oxygenated compounds could contribute to ambient total OH reactivity in the PROPET tower forest canopy. Apel et al. (2002) reported MVK, MACR, and isoprene measurement results at the PROPHET tower in 1998. The median mixing ratios of MVK, MACR, and isoprene during the daytime (10:00 a.m. to 02:00 p.m., local time) were 0.14 ppbv, 0.07 ppbv and 1.90 ppbv, respectively. Therefore, the OH reactivity ratio of MVK + MACR relative to isoprene from the ambient concentrations is 0.026. Since the PROPHET site is in the low NO_X regime (Tan et al., 2001), we applied the calculated ratios of OH reactivity from MVK + MACR and the unmeasured first generation oxidation products in low NO regime (~100 pptv of NO, S. Bertman, personal communication, 2010 and Thornberry et al., 2001) to assess potential contributions of the unmeasured first generation oxidation products of isoprene. The calculation results indicate that the unmeasured oxidation products can contribute ~7.18% (8.8% from LIM and 5.6% by MIM 2) of the isoprene contribution towards total ambient OH reactivity. This amount can explain ~8.0% (9.7% from LIM and 6.2% from MIM 2) of missing OH reactivity, reported by Di Carlo et al. (2004). In this analysis, we only consider the first generation

ACPD
11, 7781–7809, 2011

isoprene oxidation products. As noted by Karl et al. (2009), the contributions from further generation oxidation products towards total OH reactivity become significant (up to 150% of OH reactivity from isoprene) for a photochemically aged isoprene dominated air mass. Therefore, to resolve missing OH reactivity in this ecosystem our research results suggest that further investigation is needed to quantify unmeasured oxidation products of isoprene.

2 Summary and conclusion

As an activity of the CABINEX-09 field campaign, we conducted branch enclosure OH reactivity measurements on four different tree species (red oak, white pine, beech, and red maple) using PTR-MS by applying the CRM approach with a pyrrole reagent (Sinha et al., 2008). The system was set to measure OH reactivity about 75% of the time and isoprene and MT concentrations inside of the enclosure were observed about 25% of the time using PTR-MS so that we can compare total OH reactivity and calculated OH reactivity from biogenic compounds inside of the branch enclosure. The measurement from Red oak, the main isoprene emitter and white pine, the main MT emitter in the ecosystem clearly indicate that the calculated OH reactivity from isoprene and MT can explain nearly all of the measured total OH reactivity. Branch enclosure measurements of beech, which emits both isoprene and MT, also shows reasonable agreement between measured and calculated OH reactivity. Finally, branch enclosure measurements of red maple indicated a systematic discrepancy between measured and calculated OH reactivity from only isoprene and MT. However, if we include the OH reactivity from SQT (α-farnesene), detected by GC-MS from cartridge sampling, the discrepancy could be reconciled. The results indicate that contributions of ambient OH reactivity from unaccounted/unmeasured BVOC emission should be minimal during the field experiment period although additional measurements of more tree species and individuals at the site are needed to confirm this conclusion.

ACPD
11, 7781–7809, 2011

To further explore the possibility of contributions of conventionally unmeasured isoprene oxidation products such as C5, C4 hydroxycarbonyl compounds, hydroxyacetone, glyoxal, and methylglyoxal towards ambient OH reactivity, we evaluated their contributions using two isoprene oxidation schemes (LIM and MIM2) used for regional and global tropospheric chemistry models. The evaluation results indicate that the conventionally unmeasured first generation products of isoprene that are produced during the day could contribute ~20% of OH reactivity from ambient isoprene. This can be interpreted to account for ~22% of the missing OH reactivity, reported in this ecosystem by Di Carlo et al. (2004). Karl et al. (2009) pointed out that more photochemically aged air masses have even more significant contributions of OVOC to total OH reactivity, so the contribution certainly can be even greater. These analyses indicate that we need to quantify these unconstrained isoprene oxidation products in order to constrain missing OH reactivity at this forest site. As Peeters and Muller (2010) claimed from their theoretical studies, different laboratory conditions, especially NO level, can cause different distributions of oxidation products and serve as a guideline for oxidation mechanism development. This, therefore, suggests the need for more systematically NO controlled laboratory experiments along with better calibration synthesis methods. In addition, the HO_2–RO_2 ratio, which makes significant differences in oxidation product distributions (Navarro et al., 2010), should be very carefully considered in controlled laboratory experiments and interpreted for atmospheric implications (Paulot et al., 2010). This effort should be combined with the effort to characterize primary BVOC emission such as sesquiterpenes, which may contribute to total OH reactivity in some ecosystems.

Acknowledgements. We are grateful to M. A. Carroll and University of Michigan Biological Station for use of the PROPHET tower facility. We thank Tiffany Duhl for her assistance in analyzing cartridge samples. The National Center for Atmospheric Research is operated by the University Corporation for Atmospheric Research under sponsorship from the US National Science Foundation. Any opinions, findings and conclusions or recommendations expressed in this publication are those of the authors and do not necessarily reflect the views of the National Science Foundation.

ACPD
11, 7781–7809, 2011

References

Apel, E. C., Riemer, D. D., Hills, A., Baugh, W., Orlando, J., Faloona, I., Tan, D., Brune, W., Lamb, B., Westberg, H., Carroll, M. A., Thornberry, T., and Geron, C. D.: Measurement and interpretation of isoprene fluxes and isoprene, methacrolein, and methyl vinyl ketone mixing ratios at the PROPHET site during the 1998 intensive, J. Geophys. Res.-Atmos., 107, 4034, doi:10.1029/2000JD000225, 2002.

Bouvier-Brown, N. C., Holzinger, R., Palitzsch, K., and Goldstein, A. H.: Large emissions of sesquiterpenes and methyl chavicol quantified from branch enclosure measurements, Atmos. Environ., 43, 389–401, 2009.

Di Carlo, P., Brune, W. H., Martinez, M., Harder, H., Lesher, R., Ren, X., Thornberry, T., Carroll, M. A., Young, V., Shepson, P. B., Riemer, D., Apel, E., and Campbell, C.: Missing OH reactivity in a forest: Evidence for unknown reactive biogenic VOCs, Science, 304, 722–725, 2004.

Dibble, T. S.: Intramolecular hydrogen bonding and double H-atom transfer in peroxy and alkoxy radicals from isoprene, J. Phys. Chem. A, 108, 2199–2207, doi:10.1021/JP0306702, 2004a.

Dibble, T. S.: Prompt chemistry of alkenoxy radical products of the double H-atom transfer of alkoxy radicals from isoprene, J. Phys. Chem. A, 108, 2208–2215, doi:10.1021/JP0312161, 2004b.

Goldstein, A. H. and Galbally, I. E.: Known and unexplored organic constituents in the earth's atmosphere, Environm. Sci. Technol., 41, 1515–1521, 2007.

Guenther, A., Hewitt, C. N., Erickson, D., Fall, R., Geron, C., Graedel, T., Harland, R. J., Klinger, L., Lerdau, M., Mckay, M., Pierce, T., Scholes, B., Steinbrecher, R., Tallamraju, R., Taylor, J., and Zimmerman, P.: A global model of natural volatile organic compound emission, J. Geophys. Res., 100, 8873–8892, 1995.

IPCC: Climate change 2007-syntesis report, Geneva, Switzerland, 2007.

Karl, T., Guenther, A., Turnipseed, A., Tyndall, G., Artaxo, P., and Martin, S.: Rapid formation of isoprene photo-oxidation products observed in Amazonia, Atmos. Chem. Phys., 9, 7753–7767, doi:10.5194/acp-9-7753-2009, 2009.

Kim, S., Karl, T., Guenther, A., Tyndall, G., Orlando, J., Harley, P., Rasmussen, R., and Apel, E.: Emissions and ambient distributions of Biogenic Volatile Organic Compounds (BVOC) in a ponderosa pine ecosystem: interpretation of PTR-MS mass spectra, Atmos. Chem. Phys., 10, 1759–1771, doi:10.5194/acp-10-1759-2010, 2010.

ACPD
11, 7781–7809, 2011

Kim, S., Karl, T., Helmig, D., Daly, R., Rasmussen, R., and Guenther, A.: Measurement of atmospheric sesquiterpenes by proton transfer reaction-mass spectrometry (PTR-MS), Atmos. Meas. Tech., 2, 99–112, doi:10.5194/amt-2-99-2009, 2009.

Lee, A., Schade, G. W., Holzinger, R., and Goldstein, A. H.: A comparison of new measurements of total monoterpene flux with improved measurements of speciated monoterpene flux, Atmos. Chem. Phys., 5, 505–513, doi:10.5194/acp-5-505-2005, 2005.

Lou, S., Holland, F., Rohrer, F., Lu, K., Bohn, B., Brauers, T., Chang, C.C., Fuchs, H., Hseler, R., Kita, K., Kondo, Y., Li, X., Shao, M., Zeng, L., Wahner, A., Zhang, Y., Wang, W., and Hofzumahaus, A.: Atmospheric OH reactivities in the Pearl River Delta – China in summer 2006: measurement and model results, Atmos. Chem. Phys., 10, 11243–11260, doi:10.5194/acp-10-11243-2010, 2010.

Ortega, J., Helmig, D., Guenther, A., Harley, P., Pressley, S., and Vogel, C.: Flux estimates and oh reaction potential of reactive biogenic volatile organic compounds (BVOCs) from a mixed northern hardwood forest, Atmos. Environ., 41, 5479–5495, 2007.

Paulot, F., Crounse, J. D., Kjaergaard, H. G., Kroll, J. H., Seinfeld, J. H., and Wennberg, P. O.: Isoprene photooxidation: new insights into the production of acids and organic nitrates, Atmos. Chem. Phys., 9, 1479–1501, doi:10.5194/acp-9-1479-2009, 2009.

Paulson, S. E. and Seinfeld, J. H.: Development and evaluation of photooxidation mechanism for isoprene, J. Geophys. Res., 97, 20703–720715, 1992.

Sinha, V., Custer, T. G., Kluepfel, T., and Williams, J.: The effect of relative humidity on the detection of pyrrole by PTR-MS for OH reactivity measurements, Int. J. Mass Spectrom., 282, 108–111, 2009.

Sinha, V., Williams, J., Crowley, J. N., and Lelieveld, J.: The Comparative Reactivity Method – a new tool to measure total OH Reactivity in ambient air, Atmos. Chem. Phys., 8, 2213–2227, doi:10.5194/acp-8-2213-2008, 2008.

Sinha, V., Williams, J., Lelieveld, J., Ruuskanen, T. M., Kajos, M. K., Patokoski, J., Hellen, H., Hakola, H., Mogensen, D., Boy, M., Rinne, J., and Kulmala, M.: OH reactivity measurements within a boreal forest: Evidence for unknown reactive emissions, Environ. Sci. Technol., 44, 6614–6620, 2010.

Stavrakou, T., Peeters, J., and Mller, J.-F.: Improved global modelling of HO_x recycling in isoprene oxidation: evaluation against the GABRIEL and INTEX-A aircraft campaign measurements, Atmos. Chem. Phys., 10, 9863–9878, doi:10.5194/acp-10-9863-2010, 2010.

Tan, D., Faloona, I., Simpas, J. B., Brune, W., Shepson, P. B., Couch, T. L., Sumner, A. L.,

ACPD
11, 7781–7809, 2011

Carroll, M. A., Thornberry, T., Apel, E., Riemer, D., and Stockwell, W.: HO_X budgets in a deciduous forest: Results from the prophet summer 1998 campaign, J. Geophys. Res.-Atmos., 106, 24407–24427, 2001.

Thornberry, T., Carroll, M. A., Keeler, G. J., Sillman, S., Bertman, S. B., Pippin, M. R., Ostling, K., Grossenbacher, J. W., Shepson, P. B., Cooper, O. R., Moody, J. L., and Stockwell, W. R.: Observations of reactive oxidized nitrogen and speciation of NOy during the PROPHET summer 1998 intensive, J. Geophys. Res.-Atmos., 106, 24359–24386, 2001

Taraborrelli, D., Lawrence, M. G., Butler, T. M., Sander, R., and Lelieveld, J.: Mainz Isoprene Mechanism 2 (MIM2): an isoprene oxidation mechanism for regional and global atmospheric modelling, Atmos. Chem. Phys., 9, 2751–2777, doi:10.5194/acp-9-2751-2009, 2009.

Williams, J., Poschl, U., Crutzen, P. J., Hansel, A., Holzinger, R., Warneke, C., Lindinger, W., and Lelieveld, J.: An atmospheric chemistry interpretation of mass scans obtained from a proton transfer mass spectrometer flown over the tropical rainforest of Surinam, J. Atmos. Chem., 38, 133–166, 2001.

Zhao, J., Zhang, R. Y., Fortner, E. C., and North, S. W.: Quantification of hydroxycarbonyls from OH-isoprene reactions, J. Am. Chem. Soc., 126, 2686–2687, 2004.

ACPD
11, 7781–7809, 2011

Table 1. A summary of GC-MS analysis of BVOC emissions from red oak (top panel) and white pine (bottom panel) enclosures.

Red Oak Enclosure BVOC Speciation			
Terpenoids	% abundances	Species	% Abundances
Isoprene	98.9		
Monoterpenes	1.1	α−pinene β−pinene camphene β−phellandrene limonene	24.8 25.6 11.4 20.7 18.2
White Pine Enclosure BVOC Speciation			
Terpenoids	Abundances	Species	Abundances
Monoterpenes	62.8	α−pinene β−pinene camphene limonene 3-carene	18.6 35.1 11 24.4 7.96
Oxygenated monotperpenes	37.1	linalool	100
Sesquiterpenes	1.0	α−humulene β−caryophyllene	22.7 77.3

ACPD
11, 7781–7809, 2011

Table 2. A summary of GC-MS analysis of BVOC emission from beech (top panel) and red maple (bottom panel) enclosures.

Beech Enclosure BVOC Speciation			
Terpenoids	% Abundances	Species	% Abundances
MT	94.2	α−pinene	54.0
		β−pinene	9.0
		3-carene	2.1
		d-limonene	27.8
		α−phellandreene	4.8
		bphelandrene	2.1
SQT	5.8	α−farnesene	100
Maple Enclosure BVOC Speciation			
Terpenoids	Abundances	Species	Abundances
MT	46.7	Ocimene	100
SQT	53.3	a-farnesene	100

ACPD
11, 7781–7809, 2011

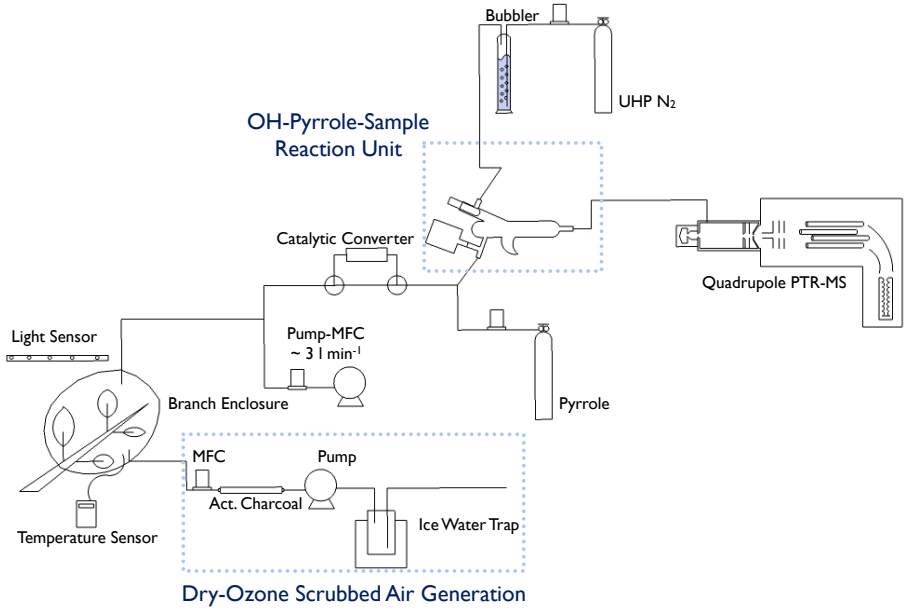

Fig. 1. A schematic diagram of the branch enclosure OH reactivity measurement system, deployed for this study.

ACPD
11, 7781–7809, 2011

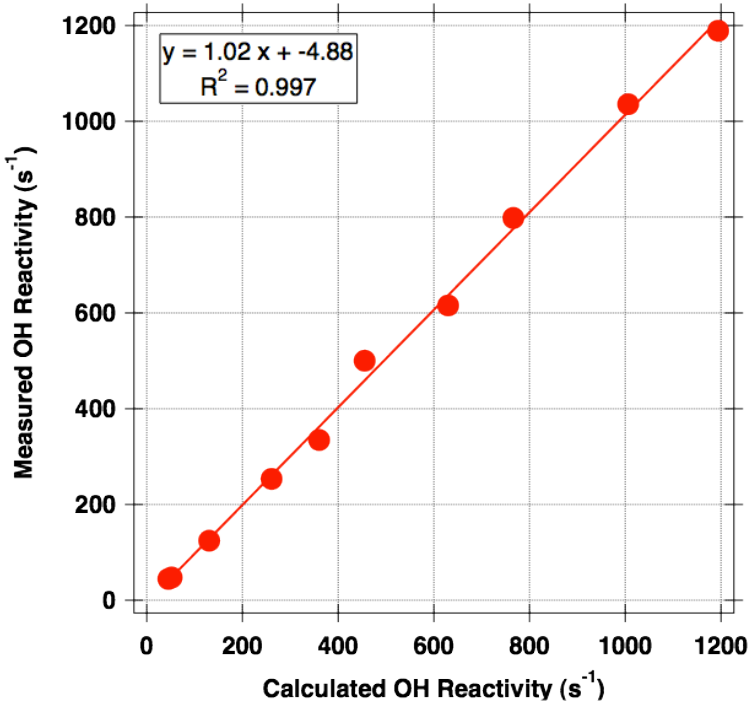

Fig. 2. Laboratory calibration results of the OH reactivity measurement system. The x-axis indicates calculated OH reactivity from standard samples and the y-axis indicates measured OH reactivity.

ACPD
11, 7781–7809, 2011

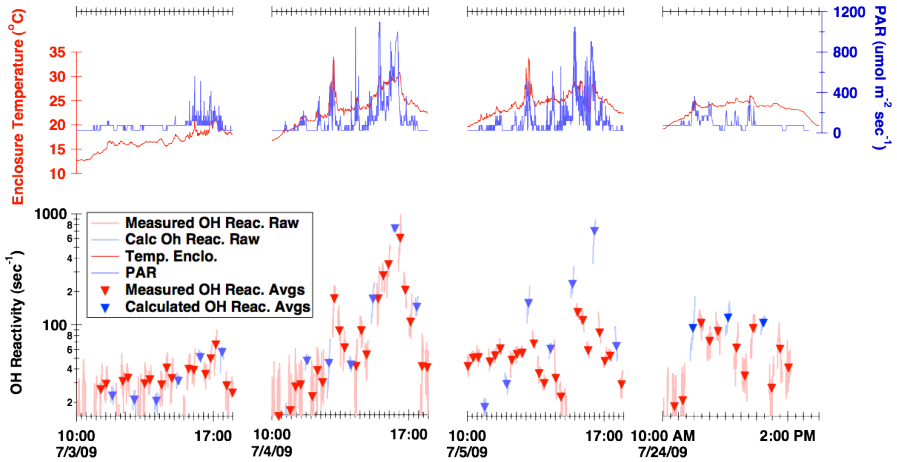

Fig. 3. Temporal variations of measured (red) and calculated (blue) OH reactivity in the bottom panel and temperature and PAR measurement in the top panel for red oak branch enclosure. (Upper Panel: PAR in the blue lines and temperature inside of branch enclosure in the red lines, Bottom Panel: measured OH reactivity in the light red lines, calculated OH reactivity in the light blue lines, 20-min averaged measured OH reactivity in the red triangles, 20-min averaged calculated OH reactivity in the blue triangles).

ACPD
11, 7781–7809, 2011

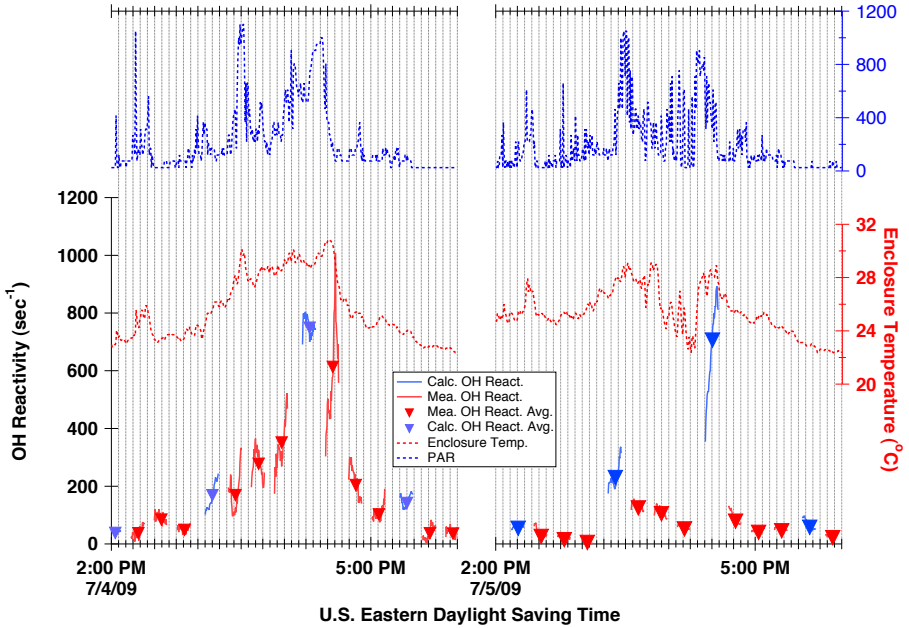

Fig. 4. Temporal variations of measured, calculated OH reactivity, enclosure temperature and PAR of 4 July and 5 July of the oak tree enclosure. (PAR in the blue dashed lines, enclosure temperature in the red dashed line, measured OH reactivity in the red lines, calculated OH reactivity in the blue lines, 20-min averaged measured OH reactivity in the red triangles, 20-min averaged calculated OH reactivity in the blue triagles).

ACPD
11, 7781–7809, 2011

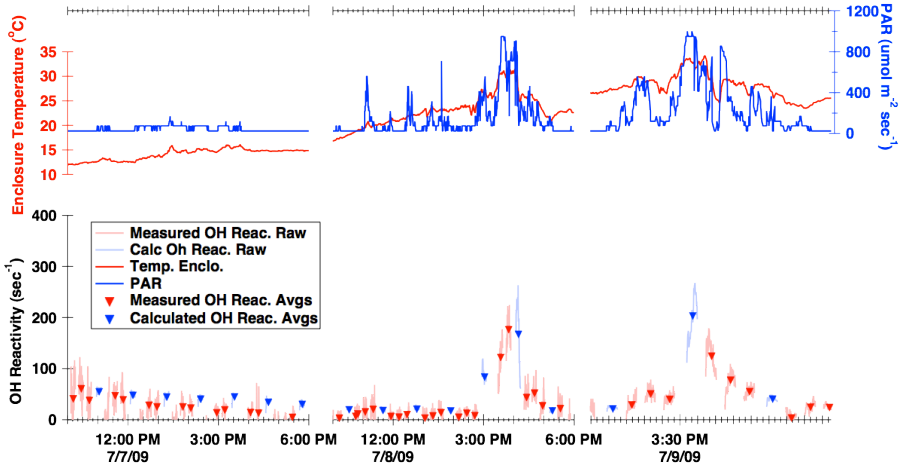

Fig. 5. Temporal variations of measured (red) and calculated (blue) OH reactivity in the bottom panel and temperature and PAR measurement in the top panel for white pine branch enclosure (Upper Panel: PAR in the blue lines and temperature inside of branch enclosure in the red lines, Bottom Panel: measured OH reactivity in the light red lines, calculated OH reactivity in the light blue lines, 20-min averaged measured OH reactivity in the red triangles, 20-min averaged calculated OH reactivity in the blue triangles).

ACPD
11, 7781–7809, 2011

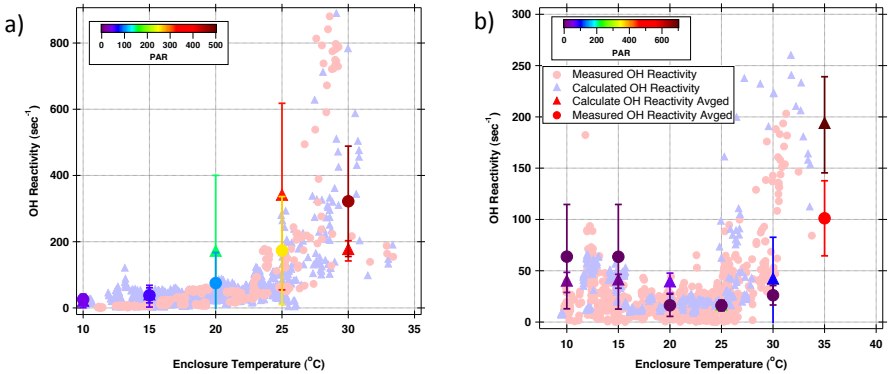

Fig. 6. Calculated (the blue triangles) and measured OH reactivity (the red circles) distribution as a function of branch enclosure temperature **(a)** red oak and **(b)** white pine branch enclosures. 5 degree C running averaged calculated and measured OH reactivity is also presented with PAR color-coding. The error bars in the plots indicate 1-sigma of the statistics.

ACPD
11, 7781–7809, 2011

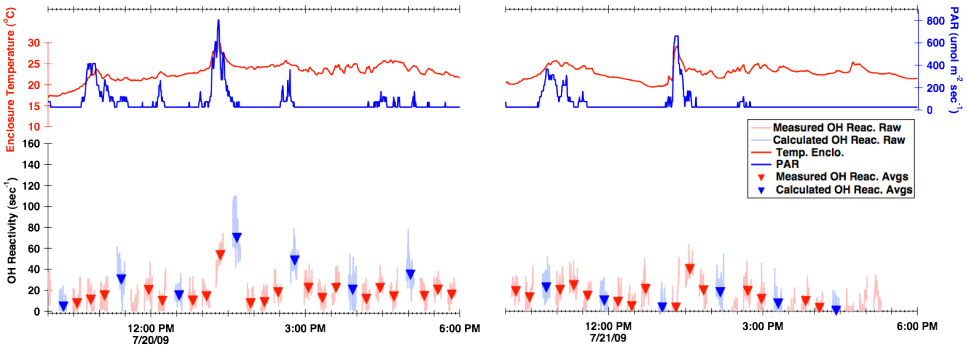

Fig. 7a. Temporal variations of measured (red) and calculated (blue) OH reactivity in the bottom panel and temperature and PAR measurement in the top panel for beech branch enclosure (Upper Panel: PAR in the blue lines and temperature inside of branch enclosure in the red lines, Bottom Panel: measured OH reactivity in the light red lines, calculated OH reactivity in the light blue lines, 20-min averaged measured OH reactivity in the red triangles, 20-min averaged calculated OH reactivity in the blue triangles).

ACPD
11, 7781–7809, 2011

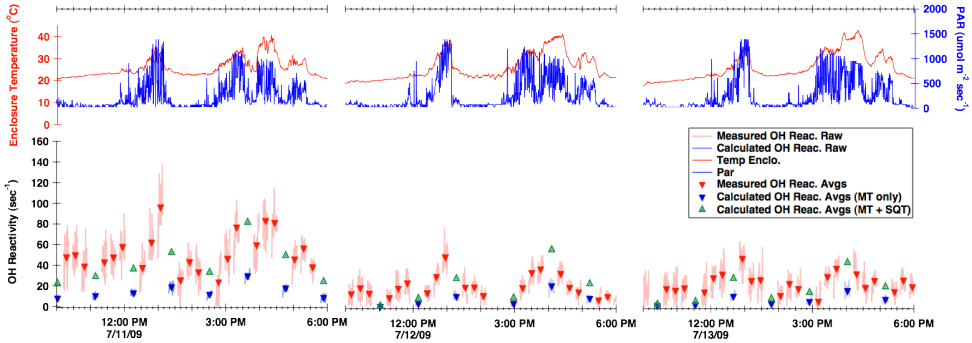

Fig. 7b. Temporal variations of measured (red) and calculated (blue) OH reactivity in the bottom panel and temperature and PAR measurement in the top panel for red maple branch enclosure. The green triangles indicate calculated OH reactivity with addition of α-farnesene emission, detected by GC-MS (see the text for detail) (Upper Panel: PAR in the blue lines and temperature inside of branch enclosure in the red lines, Bottom Panel: measured OH reactivity in the light red lines, calculated OH reactivity in the light blue lines, 20-min averaged measured OH reactivity in the red triangles, 20-min averaged calculated OH reactivity in the blue triangles).

ACPD
11, 7781–7809, 2011

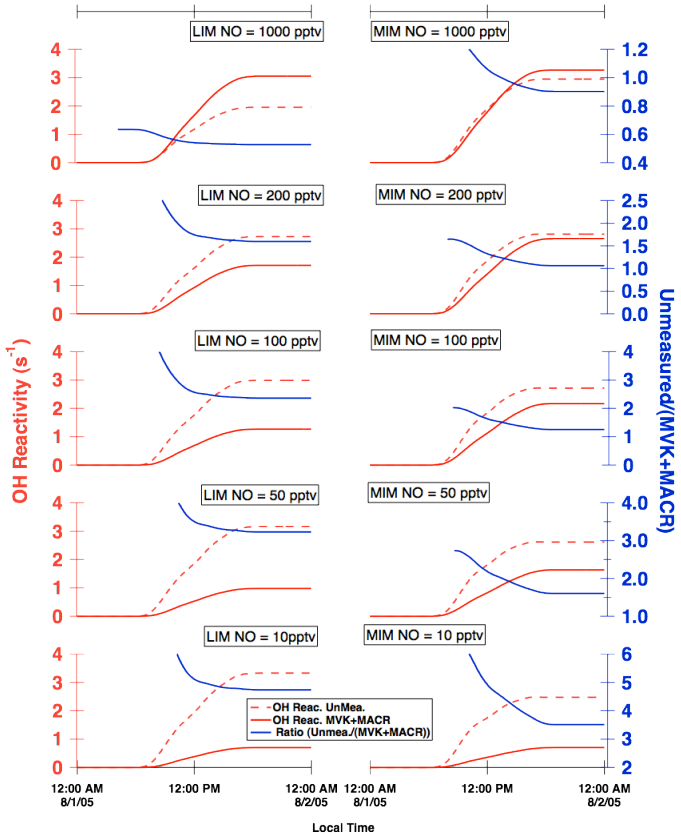

Fig. 8. Model calculated OH reactivity from MVK and MACR (the solid red line) and conventionally unmeasured isoprene first generation oxidation products (the dashed line). The blue lines in each panel indicates the temporal variations of ratios of OH reactivity from conventionally unmeasured isoprene first generation oxidation products and OH reactivity from MVK and MACR.

ACPD
11, 7781–7809, 2011